

Performance of a Conceptual Counter-flow MCHE operated on CuO-Water Nanofluid: Influence of Geometry

Avdhesh Kr. Sharma

Mechanical Engg., DCR University of Science & Technology, Murthal (Sonapat) Haryana, INDIA

ABSTRACT

Microchannel heat exchangers (MCHE) can be designed with different channel geometry such as circular, triangular, rectangular, square, trapezoidal and hexagonal. In this article, the influence of channel geometry on *thermal, hydraulic and overall performance* of counter flow MCHE operated on CuO-water nanofluid flow has been highlighted. Herein, Nusselt and Poiseuille number for different channel shapes and thermo-physical properties of CuO-water nanofluid (viz., thermal conductivity, viscosity...) have been designed either empirically or adopted from literature. Results of pumping power with trapezoidal geometry MCHE is found to be highly sensitive with nanofluid flow. Rectangular shape counter flow MCHE gives highest thermal effectiveness, while iso-triangular geometry gives best overall performance by converting the pressure energy into thermal energy.

1. INTRODUCTION

In recent years, there are growing interests in developing ultra-compact high heat removal devices commonly referred to as MEMS (Micro Electromechanical systems) such as microchannel heat exchangers, microchannels heat sinks, micromixer, microreactors and microsensors. Recent progress in nanotechnology made it possible to produce nanometer-sizes particles easily. Eastman et al [1] revealed that nanoparticles are usually oxides of high thermal conductive metals (i.e., CuO, Al₂O₃, TiO₂ etc.), having size less than 100 nm, can have stable suspension in industrial heat transfer fluids (for instance, water, ethylene glycol, or engine oil). It results in an advanced class of coolants namely *nanofluids*. These nanofluids can solve the problem of sedimentation, clogging, settling of solid-particles, scaling and erosions during heat transfer process. Due to recent advances in manufacturing technologies (i.e., etching, vapour deposition, diffusion bonding, extruded aluminum multichannel tubes,...), it is possible to construct microchannels in the range of 1 μm - 1 mm. Microchannel heat exchangers have found applications in highly specialized areas such as microelectronics cooling, aerospace, biomedical processes, metrology, robotics, telecommunications and automotive industries [2]. Utilization of nanofluids in such microchannels may further enhance heat transfer rates and pumping power for recirculation.

Numerous studies have been reported in past on nanofluid properties [3–8]. Researchers have refined the theory for effective thermal conductivity of nanofluids by accounting Brownian motion, particle aggregation and interfacial nanolayer [5, 7]. Koo and Kleinstreuer [5] defined the nanofluid thermal conductivity is a combination of static and Brownian motion part. Latter, Vajjha and Das [7] have improved the model by broadening the volumetric particle concentration range for nanofluids. On the other hand, Wong and Kurma [9] and Nguyen et al [11] have measured carefully the dynamic viscosity of several water based nanofluids for temperatures up to $\sim 70^\circ\text{C}$. They measured the viscosities for different water-based nanofluids: Al₂O₃-water and CuO

nanoparticles with 29 nm diameter. Rachkovskij et al [11] studied heat transfer in microtubes of cross flow micro heat exchanger and investigated the influence of tube size and relative length on heat transfer. Hasan et al. [2] have performed numerical simulation on various non-circular counter flow MCHE to study the effect of size and shape of channels on the thermal and hydraulic performance. Latter, an interesting comparative study on square shaped parallel flow MCHE was conducted to investigate heat transfer and fluid flow characteristics using water based nanofluids i.e., Al_2O_3 , SiO_2 , Ag and TiO_2 [12].

Literature revealed that extensive studies were conducted on microchannel heat sinks and characterization of nanofluids; the studies on two fluids MCHE are very limited. Hardly few references have been reported. It is understandable that the surface/volume ratio in microchannels is very large. Thus, the role of surface dominant factors becomes more important. On other hand, in MCHEs, replacing conventional coolant with nanofluid may further enhance the heat transfer rate. In this work, therefore, counter flow MCHE arrangement has been conceptualized with different channel geometry (viz., circular, triangular, rectangular, square, trapezoidal and hexagonal). The influence of channel geometry on the *thermal*, *hydraulic* and *overall* performance of counter flow MCHE operated on CuO-water nanofluid flow has been highlighted.

2. FORMULATION

Schematic structure of a conceptual design of counter flow MCHE with circular shape is shown in Figure 1. As explained earlier, counter flow MCHE arrangement can be expected to have various geometrical shapes (viz., circular, triangular, rectangular, square, trapezoidal and hexagonal) as shown in Figure 2. The row-wise distribution of cold flow and hot flow streams are arranged carefully in order to facilitate more surface area for heat exchange. The possible structure allowing ease in flow distribution and maximum thermal interactions with neighboring channels (are represented by the black arrows) is shown in Figure 2(a)-(e).

Following assumptions were invoked for formulation.

1. Properties are constant and flow is considered as fully developed hydraulically and thermally.
2. Heat capacities and Reynolds number on both sides are same irrespective to temperature variation and variation in concentration of CuO particles.
3. Single element channel (cell) represents the performance of MCHE.
4. Effective wall thickness of different shape element cell is assumed to be fixed.
5. Pumping efficiency in baseline water flow and nanofluid flow is essentially invariant.

For comparative analysis of influence of geometry, a constant volume or cross-section area of each elemental cell (which covers flow area and covering half wall thick area) is considered as input information. The enlarged view of typical hexagonal element cell for visualization of flow area, cell area and half wall thick area is represented in fig. 3

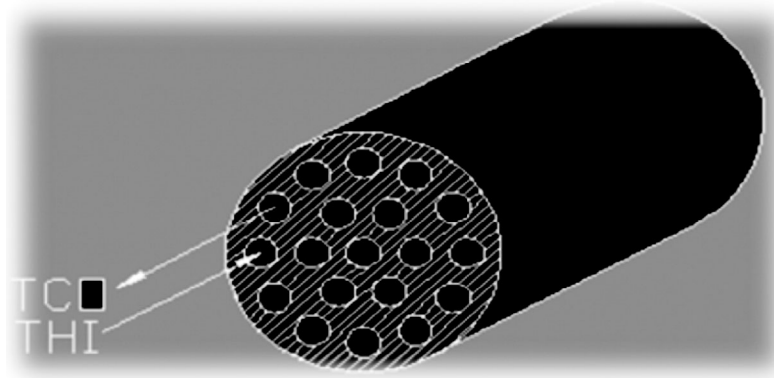


Figure 1. Conceptual design of counter flow.

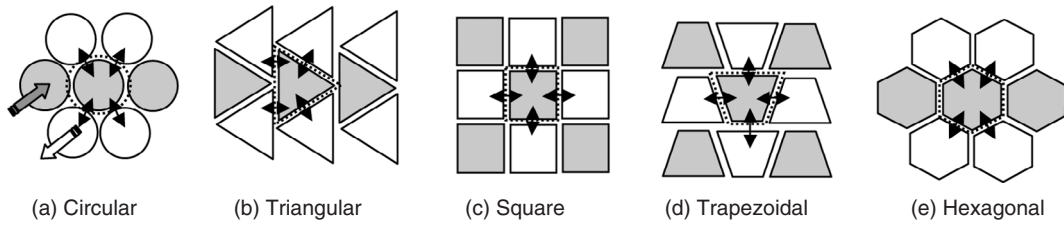


Figure 2. Possible flow distribution for different shape counter flow MCHE to enhance thermal interactions with neighboring channels (shaded area represents in-going flow, while un-shaded region designate to out-coming direction).

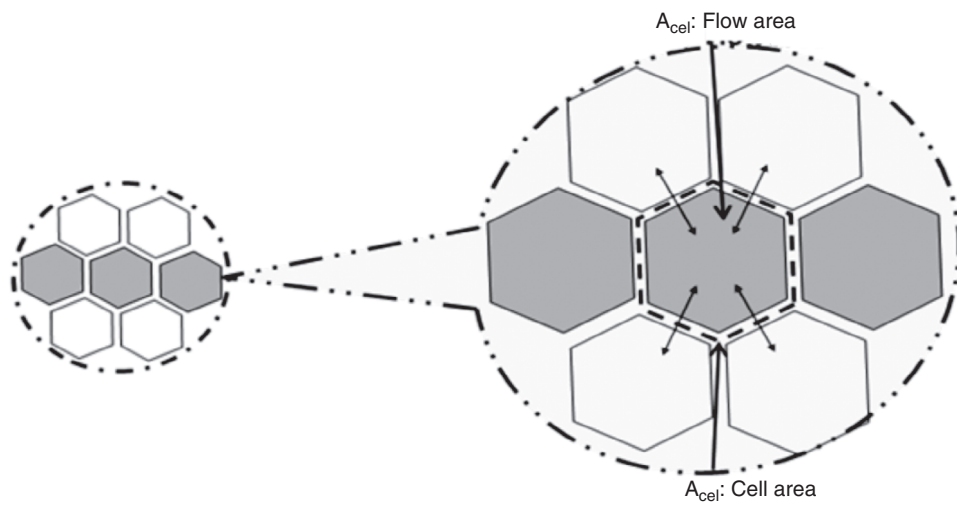


Figure 3. Enlarged view of hexagonal element cell covering flow area, cell area and half wall thick area (black arrows represent to thermal interaction with counter part neighbouring channels).

2.1. Hydraulic diameter

For each elemental cell, the volume (V_{cel}), length (L_{cel}) and effective wall thickness (t) supplied as input information. These values are fixed for each geometrical element cell. Therefore, the cell area (A_{cel}) can be obtained as V_{cel}/L_{cel} . If wall thickness of each cell-geometry is assumed to be uniform; the flow area A_c for each cell (channel) can be known. This gives hydraulic diameter (D_h) for each microchannel element cell as

$$D_{h,j} = 4A_c/p_j \tag{1}$$

Here p is wetted perimeter of microchannels, subscript j designate to circular, triangular, rectangular, square, trapezoidal and hexagonal shapes, respectively.

2.2. Performance of counter flow MCHE

2.2.1. Hydraulic performance

Attention in this work is limited to laminar flow regime only, as fully turbulent regime is seldom encountered in microchannel heat transfer applications. For given Reynolds number, the pumping power (PP) of each MCHE can be written as

$$PP_j = A_c V_b \Delta P_j / \eta_{pump} \tag{2}$$

Table 1. Poiseuille number (Po) for geometries.

Geometry	Poiseuille number	Reference
Circle	64.00	[13]
Triangular	53.33	[13]
Square	56.91	[13]
Rectangular	$4(4.7 + 19.64G)$, $G = (\alpha^{-2} + 1)/(\alpha^{-1} + 1)^2$, $\alpha =$ shape factor	[14]
Trapezoidal	$4(11.43 + 0.8e^{2.67\beta})$, $\beta =$ shape factor	[15]
Hexagonal	60.22	[13]

$$\Delta P_j = \left[K_{ent} + \frac{f_j L}{D_h} + K_{dev} \right] \rho V_b^2 / 2 \quad (3)$$

Where $V_b = \mu_{eff} Re_{Dh} / \rho_{eff} D_h$ and η_{pump} is pump efficiency, K is the pressure drop parameters and subscripts ent and dev corresponds to entrance and developing flow, respectively. f is friction factor for j^{th} microchannel which can be calculated in terms of Poiseuille number Po as ($f_j = Po_j / Re_{Dh}$), which for various geometries has been listed in table 1.

The friction factors of nanofluid with increasing volumetric particle concentration were compared [16] and found no change in Poiseuille number (Po). Thus, in this work, the same expression of Po for baseline water flow is employed for CuO-water nanofluid flow also.

2.2.2. Thermal performance

If heat capacities of both streams in counter flow microchannel heat exchanger are equal, the heat exchanger effectiveness can be defined as

$$\varepsilon = \frac{(Th_i - Th_o)}{(Th_i - Tc_i)} = \frac{(Tc_o - Tc_i)}{(Th_i - Tc_i)} \quad (4)$$

Where outlet temperature can be written in terms of inlet temperatures as

$$Th_o = Th_i - (Th_i - Tc_i)\phi \quad (5)$$

$$Tc_o = Tc_i + (Th_i - Tc_i)\phi \quad (6)$$

$$\text{Where } \phi = \frac{U_j P_j L}{U_j P_j L + \rho_{eff} A_c V_b C p_{eff}}$$

The overall heat transfer coefficient U can be written as

$$\frac{1}{U_h A_s h} = \frac{1}{U_c A_s c} = \frac{1}{h_c A_s c} + \frac{t}{k \cdot A_c} + \frac{1}{h_h A_s h} \quad (7)$$

Here k and h are the thermal conductivity of material and heat transfer coefficients. ' t ' is average thickness of microchannel wall, A_c and A_s are flow area and surface area for heat transfer, respectively. Due to similarity on both sides, h_h will be equal to h_c . For laminar flow, Chein and Huang [14] expression of Nusselt number for nanofluids is used.

$$Nu = 0.4328 \left(1.0 + 11.285 \varphi^{0.754} Pe_d^{0.218} \right) Re^{1/3} Pr^{0.4} \quad (8)$$

Here φ is volumetric particle concentration and Peclet number and Prandtl number can be defined as $Pe_d = u_b d_p / \alpha_{eff}$ and $Pr = \mu_{eff} / \rho_{eff} \alpha_{eff}$ respectively. Effective thermal diffusivity is $\alpha_{eff} = k_{eff} / (\rho \cdot Cp)_{eff}$ and properties of CuO-water nanofluid are described in next section.

2.2.2. Overall performance

For comparing the overall performance of a counter flow MCHE, a link of thermal and hydraulic performance parameters is needed. Hasan et al [2] used overall performance parameter index for MCHE in terms of heat transferred between the fluid streams q and pumping power PP as

$$\eta_j = q_j / PP_j \quad (9a)$$

Another form of performance index in terms of effectiveness and total pressure drop has been used to define overall heat exchanger performance

$$\eta_j^* = \varepsilon_j / \Delta P_j \quad (9b)$$

Hasan et al [2] quoted that both can be used to obtain practical and physical indication about the exchangers overall performance. In the present work, eqn. (9a) is employed.

2.3. Properties of CuO-water nanofluid

2.3.1. Effective specific heat and density

The specific heat of nanofluid can be described by *mass-averaged expression* satisfying *thermal equilibrium* conditions between the nanoparticles and liquid phase [17] as

$$(\rho Cp)_{eff} = (1 - \varphi) \cdot (\rho Cp)_{bf} + \varphi \cdot (\rho Cp)_p \quad (10)$$

Whereas the density of nanofluids can be described using the *liquid-particle mixture theory* as

$$\rho_{eff} = \varphi \cdot \rho_p + (1 - \varphi) \cdot \rho_{bf} \quad (11)$$

2.3.2. Effective thermal conductivity

There are numerous model of thermal conductivity of nanofluid. The effective thermal conductivity of CuO-water nanofluid can be described by a combination of two terms - (i) conventional static term and (ii) Brownian motion contribution. Finally we can express,

$$k_{eff} = k_{static} + k_{brownian} \quad (12)$$

For prediction of thermal conductivity of CuO-water nanofluids, a basic structure of well-tested Koo and Kleinstreuer model [16] is used. The static part is based on Maxwell's model, while the dynamic part is based on *translational time-averaged speed* due to the Brownian effect [16] as

$$k_{static} = \frac{k_p + 2k_{bf} - 2(k_{bf} - k_p)\varphi}{k_p + 2k_{bf} + (k_{bf} - k_p)\varphi} k_{bf} \quad (13)$$

$$k_{brownian} = 5 \times 10^{-4} \beta \varphi \rho_{bf} C_{p_{bf}} f \sqrt{\frac{k_b T}{\rho_p d_p}} \quad (14)$$

In eqn.(14), β and f were model empirically to account for the hydraulic interaction among the Brownian motion induced fluid parcels and the particle interaction due to the particle interaction potential to encapsulate the strong temperature dependence. In order to broaden the volumetric particle concentration range ($1\% \leq \varphi \leq 6\%$) and temperature range ($298 \leq T \leq 363$ K) for CuO-water nanofluid, the empirical relations as reported by Vajjha and Das [7] is employed.

$$\beta = 9.881(100\varphi)^{-0.9446} \quad (15)$$

$$f = (2.8217 \times 10^{-2} \varphi + 3.917 \times 10^{-3}) \left(\frac{T}{273} \right) - (3.0669 \times 10^{-2} \varphi + 3.91123 \times 10^{-3}) \quad (16)$$

2.3.3. Effective viscosity

A very few experimental data (widely scattered) on viscosity of CuO-water nanofluid is available in open literature. In this work, therefore, experimental data on CuO-water nanofluid with particle size of 29 nm [10], is employed to correlate the effective viscosity in following form

$$\mu_{eff} = 0.1472475 + \frac{19.5}{T} + 0.0223125\varphi^2 + \frac{11.06}{T^2} + 8.45175567 \frac{\varphi}{T^2} \quad (17)$$

The validity of above expression is limited to the temperature and particle volume concentration range of 20–58.7°C and 0–9%, respectively (maximum error range of $\pm 5\%$). The viscosity of base fluid (i.e., distilled water) can be obtained following the expression as reported in [10].

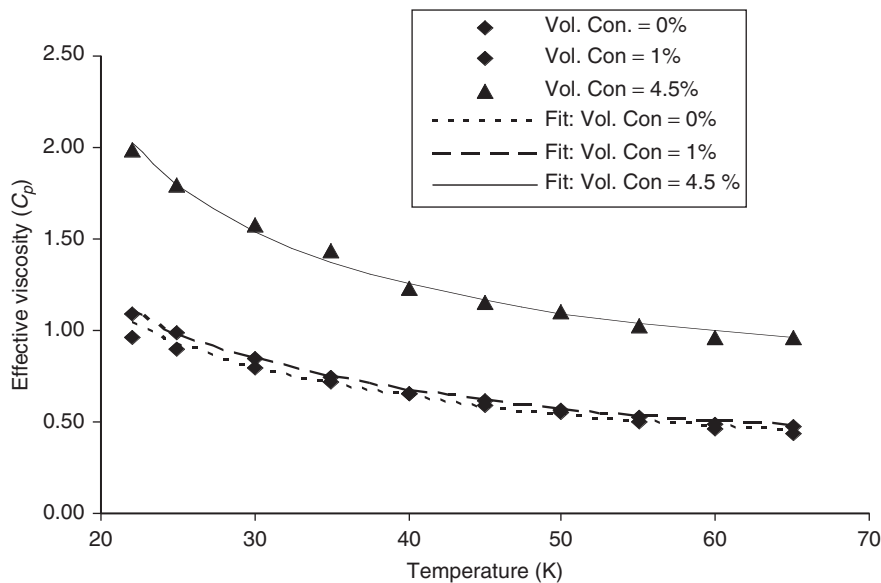


Figure 4. Comparison of curve fit (eqn. 17) with exp. of Nguyen et al [10] for effective viscosity of CuO-water nanofluid of particle size 29 nm (points- exp., line- curve fit).

$$\mu_{bf} = 10^{-7} \times \exp\left(\frac{1.12646 - 0.039638T}{1 - 0.00729769T}\right) \quad (18)$$

3. RESULTS AND DISCUSSION

For analysis, the inlet temperatures of hot and cold streams are assumed to be 293 K and 373 K. Since fully turbulent regime is seldom encountered in microchannel heat transfer applications and transition of flow regime in microchannels occurs much early (i.e., $Re = 1000$) compared with conventional channels [2]. Therefore, in this work, Reynolds number range was varied only from 20 to 900 (to ensure flow is essentially in laminar regime) through the various MCHEs operated on baseline water and CuO-water nanofluid. The flow velocities and hence mass flow rates are obtained from Re itself. The volume of cell and length of MCHE, and wall thickness has been fixed at $2.5 \times 10^{-10} \text{ m}^3$, 10 mm and 50 μm , respectively, following Hasan et al [2]. It gives flow area and perimeter of channel to predict thermal, hydraulic and overall performance. Particularly, iso-triangular shape is considered, while for both rectangular and trapezoidal shape, the aspect ratio is fixed at 0.5. The value of perimeter, hydraulic diameter and cross-section shape number of the various channel geometry is listed in Table 2. For comparison with CuO-water nanofluid flow, the volumetric concentration and particle size are kept at 4% and 29 nm, respectively. The properties of working fluid and nanoparticle material are listed in Table 3. With these inputs, simulations are run to predict hydraulic, thermal and overall performance of different geometry of MCHE. Hydraulic performance for counter flow MCHE of each channel shape (viz., circular, triangular, rectangular, square, trapezoidal and hexagonal) has been described as pressure drop or pumping power. Pump efficiency is fixed at 80% for all channel geometries. Trends of pumping power for each channel shape and for pure water and CuO-water nanofluid flow are plotted in Figures 5–6.

For both cases of pure water flow and CuO-water nanofluid flow, the pumping power increases with Reynolds number for each shape, as expected. Trapezoidal geometry shows the marked increase in pumping power, while circular shape gives the lowest pumping power. The skin friction across the channel increases with surface area and fluid viscosity, in contrast to hydraulic diameter. Trapezoidal shape offers both high perimeter and low hydraulic diameter. Thus, sharp pressure drop can be expected (refer Table 2). Moreover, nanofluids gives high viscosity values resulting in very high pressure drop or pumping power for trapezoidal shape MCHE flooded with CuO-water nanofluid, in contrast to

Table 2. Perimeter and hydraulic diameter of different channel geometries.

Geometry	Perimeter (mm)	Hydraulic diameter(mm)	Cross-section shape number
Circle	0.403	0.128	1.000
Triangular	0.228	0.044	0.605
Square	0.432	0.108	0.785
Rectangular	0.459	0.102	0.698
Trapezoidal	0.481	0.082	0.536
Hexagonal	0.415	0.119	0.907

Table 3. Properties of working fluid and nanoparticle material [6].

Conductivity Fluid/material	Density (kg/m ³)	Specific heat (J/kgK)	Th (W/mK)
CuO	6500	540	17.65
Cu	8933	385	401

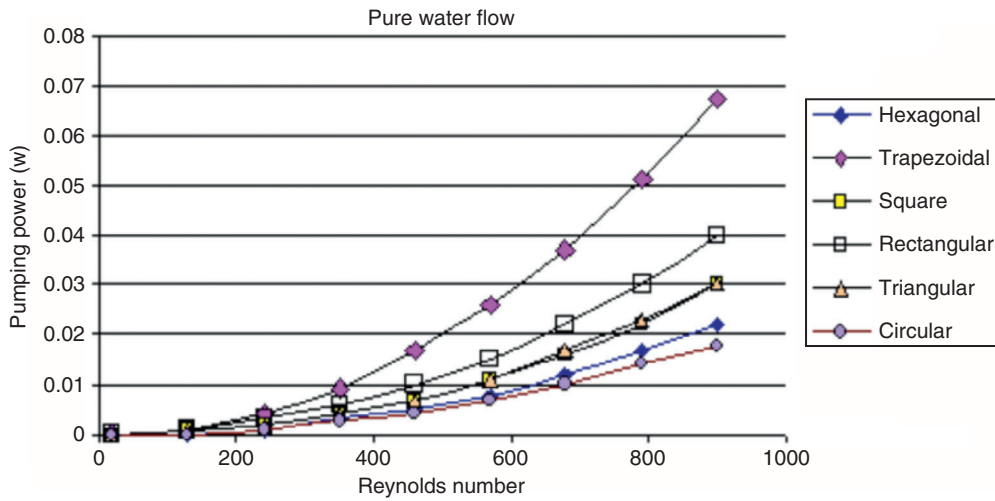


Figure 5. Effect of geometry on pumping power, pure water flow.

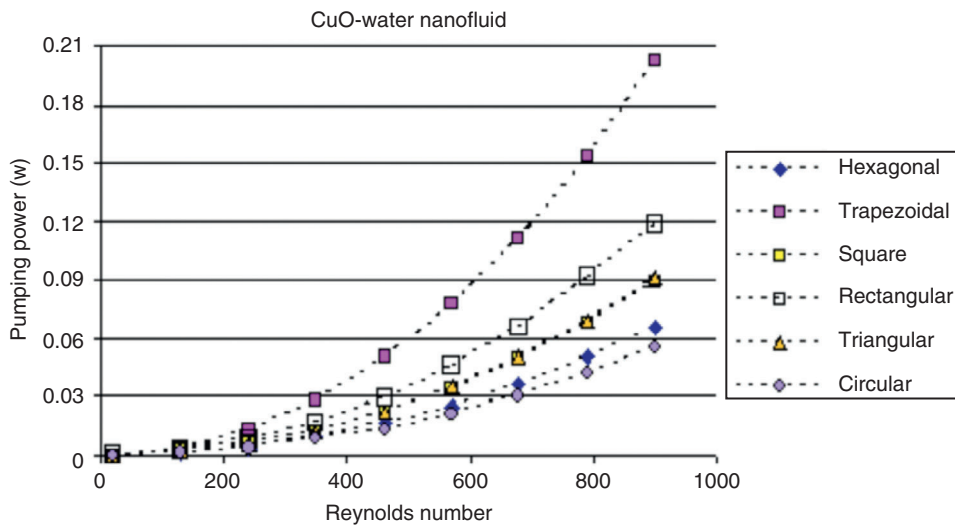


Figure 6. Effect of geometry on pumping power, CuO-water nanofluid.

circular MCHE which have highest hydraulic diameter. For stationary or mobile systems high pressure drop may be tolerated at the cost of higher heat transfer; in contrast in space applications, the pressure drop must be minimized to avoid payload costs (i.e., pump, motor etc.)[2].

For counter flow MCHEs, thermal performance is described in terms of thermal effectiveness. Effects of Reynolds number for pure water flow and CuO-water nanofluid are plotted by Figures 7–8. It can be observed clearly that the counter flow MCHE effectiveness decreases with Reynolds number for both cases. Thermal effectiveness of circular shape geometry is lowest, while rectangular shape gives highest trends in laminar flow regime. For nanofluid flow, as shown in fig. 8, the effectiveness improves considerably as compared to baseline pure water flow. Thermal effectiveness for circular microchannel heat exchanger improves from 5–74% for increasing Reynolds number from 20 to 900.

For CuO-water nanofluid flow, higher effectiveness is expected since thermal conductivity and heat transfer coefficient improves with volumetric particle concentration, which in turn increases heat

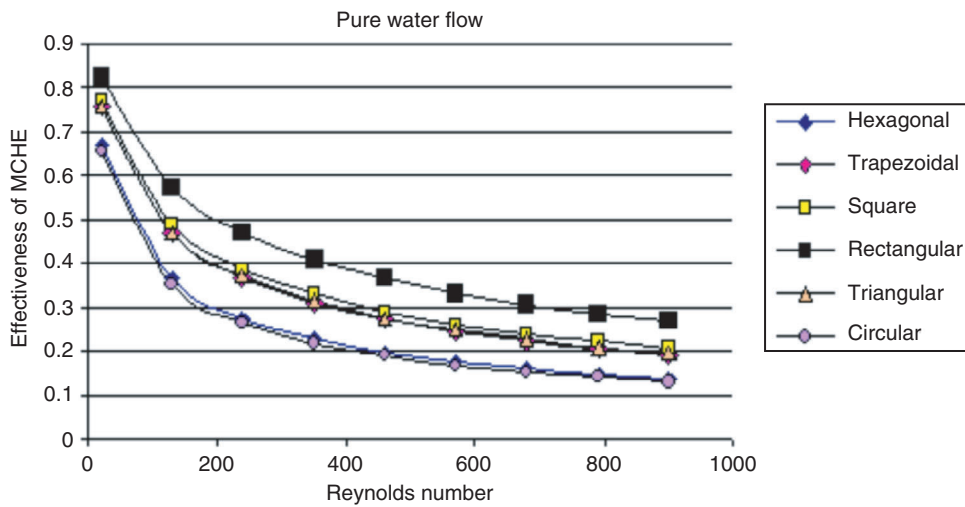


Figure 7. Effect of geometry on effectiveness, Pure water flow.

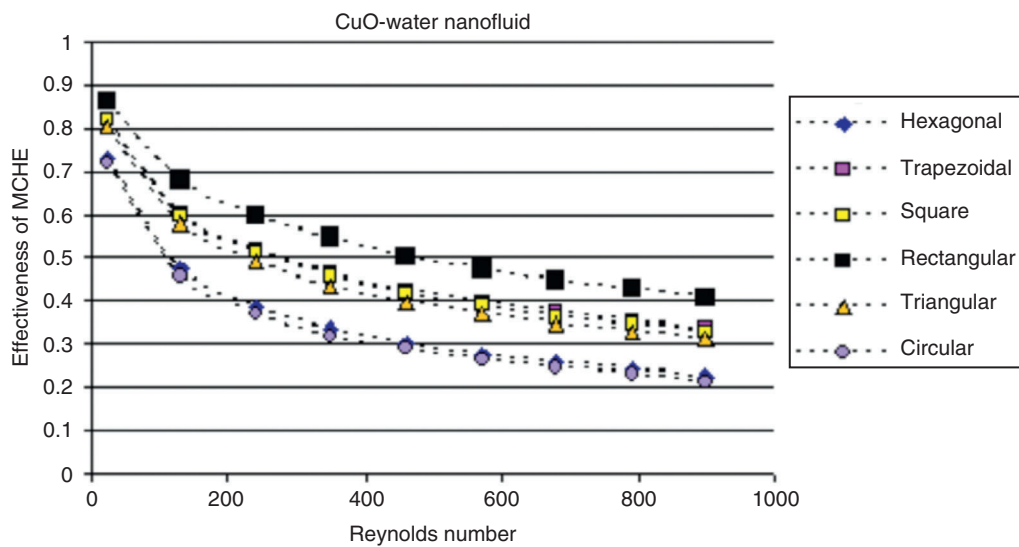


Figure 8. Effect of geometry on effectiveness, CuO-water nanofluid.

transfer. Effectiveness of rectangular shape with aspect ratio of 0.5 is expected to be highest as it gives highest heat transfer coefficient and utilize full perimeter for heat exchange (refer Figure 2c). In contrast to it, circular geometry, which shows lowest effectiveness, due to lowest heat transfer coefficient and it utilizes only 2/3 circumferential area for heat exchange.

Overall performance index is established to link between thermal and hydraulic performance counter flow MCHE (eqn. 9). The trends for performance index for each channel shape is plotted in Figures 9–10. The overall performance of microchannel heat exchanger decreases from 89 to 28% for increasing Reynolds number from 20 to 900. Triangular shape MCHE gives best overall performance, while trapezoidal shape performs worst. Iso-triangular shape MCHE utilizes full perimeteric surface area for heat transfer without any severity of pumping power, thus based on above study, iso-triangular shape can be recommended for counter flow MCHE. The role of nanofluid may not be so encouraging (Figure 10).

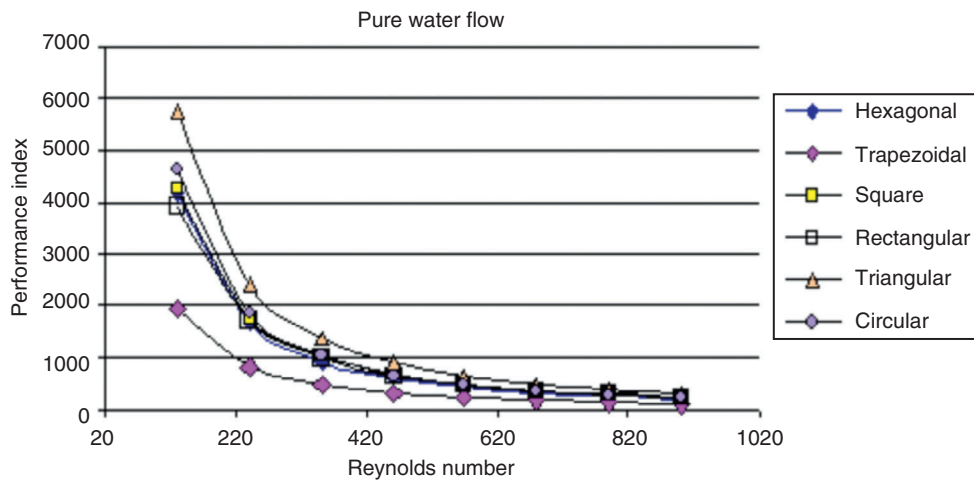


Figure 9. Effect of geometry on overall performance, Pure water flow.

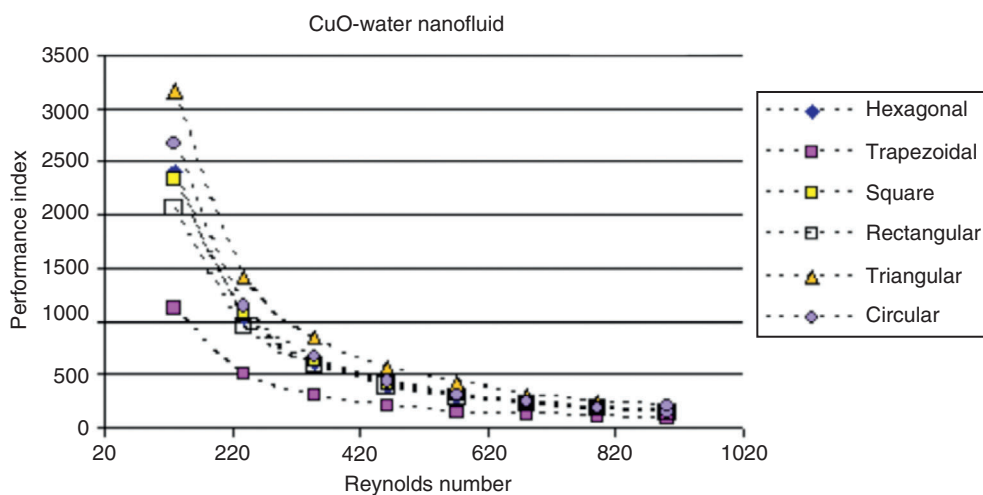


Figure 10. Effect of geometry on overall performance, CuO-water nanofluid.

4. CONCLUSION

A framework for comparison of overall performance of various geometry CFMCHE (for given volume) linking thermal and hydraulic performance, along with the influence of CuO-water nanofluid flow has been critically presented. For Nanofluid, thermo-physical properties, Nusselt number (Nu) and Poiseuille number (Po) for each channel shape have been designed either empirically or adopted from open literature.

Results of pumping power through various MCHEs with nanofluid flow are found to be more sensitive as compared to baseline water flow. Trapezoidal counter flow MCHE shows marked increase in pumping power, while circular geometry gives lowest trends for both cases of baseline water flow and CuO-water nanofluid flow. Thermal effectiveness of counter flow MCHE improves with CuO-water nanofluid flow for all shapes. Rectangular shape geometry with aspect ratio of 0.5 performs best as it offers highest heat transfer coefficient and utilize full surface area for heat exchange, while circular shape performs worst, as it utilizes only 2/3 circumferential area for heat exchange and offers lowest heat transfer coefficient.

Iso-triangular shape counter flow MCHE gives best overall performance, while trapezoidal shape performs worst (due to very high pumping power). Isosceles triangular shape MCHE utilizes full perimeter for heat transfer, while pumping power is not so severe. Isosceles triangular shape is recommended (from all above cases) for developing the microscale cooling devices for current and future heat removal applications.

REFERENCES

- [1] Eastman J.A., Choi U.S., Lee S., Thopson L.J., Lee A.S., Enhanced Thermal Conductivity through the development of nanofluids: Proceedings of *conference: Fall meeting of the Materials Research Society (MRS)*, Boston, USA, 1996, 3–11.
- [2] Hasan M.I., Rageb A.A., Yaghoubi M., Homayoni H., Influence of channel geometry on the performance of a counter flow microchannel heat exchanger. *Int. J. of Thermal Sc.*, 48, 2009, 1607–18.
- [3] Koblinski P., Prasher R., Eapen J., Thermal conductance of nanofluids: is the controversy over? *J. of Nanoparticles Research*, 2008, 10, 1089–97.
- [4] Lee S., Choi S.U.S., Li S., Eastman J.A., Measuring thermal conductivity of fluids containing oxide nanoparticles, *Journal of Heat Transfer*, 121, 1999, 280–88.
- [5] Koo J. and Kleinstreuer C., A new thermal conductive model for nanofluids. *J. of Nanoparticles Research*, 6, 2004, 577–88.
- [6] Jang S.P., Choi S.U.S., Effect of various parameters on nanofluids thermal conductivity, *Journal of Heat Transfer*, 129, 2007, 617–623.
- [7] Vajjha R.S., Das D.K., Experimental determination of thermal conductivity of three nanofluids and development of new correlation, *Int. J. of Heat & Mass transfer*, 2009, 4675–82.
- [8] Sharma Avdhesh Kr., Singh A., Model development for effective thermal conductivity and dynamic viscosity of Alumina-water nanofluid, Paper code μ FLU08-253, *In: Proceeds. of the 1st European Conf. on Microfluidics*, Bologna, Dec. 10–12, 2008.
- [9] Wong K.V., Kurma T., Transport properties of alumina nanofluids, *Nanotechnology*, 19, 2008, 345702 (8p.)
- [10] Nguyen C.T., Desgranges F., Roy G., Gallanis N., Mare T., Boucher S., Mintsa H. A., Temperature and particle- size dependent viscosity data for water- based nanofluids-Hysteresis phenomenon. *Int. J. of Heat and Fluid Flow*, 28, 2007, 1492–506.
- [11] Rachkovskij D.A., Kussul S.A., Talayev S.A., Heat exchange in short microtubes and micro heat exchangers with low hydraulic losses, *In: Microsystems Technologies*, 4, Springer, 1998, 151–158.
- [12] Mohammed H.A., Bhaskaran G., Shuaib N.H., Abu-Mulaweh H.I., Influence of nanofluids on parallel flow square microchannel heat exchanger performance, *Int. Comm. in heat and mass transfer*, 38, 2011, 1–9.
- [13] Kakac S., Liu H., *Heat Exchangers: Selection, rating and thermal design*, 2nd Ed., CRC Press, 2002.
- [14] Chein R., Huang G., Analysis of microchannel heat sink performance using nanofluids, *Applied Thermal Engg.*, 25, 2005, 3104–14.
- [15] Li J., Kleinstreuer C., Thermal performance of nanofluid flow in microchannels, *Int. J. of Heat and Fluid flow*, 29, 2008, 1221–32.
- [16] Li J., *Computational Analysis of Nanofluid Flow in Microchannels with Applications to Micro-heat Sinks and Bio-MEMS*, Ph.D. Thesis, Mechanical Engg., North Carolina State University, Raleigh, 2008.
- [17] Xuan Y, Roetzel W., Conception for heat transfer correlation of nanofluids. *Int. J. Heat Mass Transfer*, 43, 2000, 3701–7.
- [18] Koo, J. Kleinstreuer C., Laminar nanofluid flow in microsheet-shinks. *Int. J. Nanoparticle Res.*, 48, 2005, 2652–61.

